Journal of Power Sources 196 (2011) 6756–6761

Contents lists available at ScienceDirect

Journal of Power Sources

journal homepage: www.elsevier.com/locate/jpowsour

# Interfacial resistance of the $LiFePO_4$-C/PEO-LiTFSI composite electrode for dry-polymer lithium-ion batteries

K. Hanai*, M. Ueno, N. Imanishi, A. Hirano, O. Yamamoto, Y. Takeda

*Department of Chemistry, Faculty of Engineering, Mie University, 1577 Kurimamachiya-cho, Tsu, Mie 514-8570, Japan*

ARTICLE INFO

*Article history:*
Received 11 August 2010
Received in revised form 21 October 2010
Accepted 23 October 2010
Available online 3 November 2010

*Keywords:*
Polymer electrolyte
PEO
$LiFePO_4$
Interface
Resistance

ABSTRACT

The interfacial resistance between the composite electrode and PEO-based solid polymer electrolyte was examined using two different symmetrical cells and AC impedance measurements in the temperature range of 30–60 °C. Of the four major resistance components identified in our previous study, three components due to the resistances of the polymer electrolyte and the charge transfer resistance between $LiFePO_4$-C and the electrolyte were assigned; however, one resistance component, in the medium frequency range has not yet been assigned. In this report, the medium frequency range resistance component was investigated using a symmetrical cell with composite electrodes composed of active and inactive materials ($LiCoO_2$, $LiMn_2O_4$ and $SiO_2$), solid polymer electrolyte, and carbon fiber as an electron conductor. The resistance was not affected by the carbon coating in $LiFePO_4$-C and the conductive carbon additive (VGCF). An electron blocking cell was also prepared and the resistance was measured in the temperature range of 30–60 °C to confirm the effect of the electrode thickness and the electrode composition. The resistance was not affected by the thickness, and decreased with decreasing PEO-LiTFSI electrolyte content in the composite electrode. However, no significant change in the activation energy was evident with the change in the electrode composition.

## 1. Introduction

Dry-polymer electrolyte lithium ion batteries (LPBs) are considered to be the best candidate to improve the safety, energy density and cost of conventional liquid electrolyte systems, because the solid polymer electrolyte (SPE) offers advantages including high durability and flexibility for cell design [1,2]. The polymer material most commonly used for SPE is poly(ethylene oxide)-$Li(CF_3SO_2)_2N$ (PEO-LiTFSI). The PEO-LiTFSI electrolyte exhibits practical lithium ion conductivity above 60 °C [3]. However, the stability window of PEO does not exceed 4 V (vs. $Li/Li^+$) [4]. Therefore, typical cathode materials for lithium ion batteries, such as $LiCoO_2$ and $LiMn_2O_4$, cannot be used with PEO-LiTFSI. $LiFePO_4$-carbon composites have been studied as ideal cathode materials for LPBs, due to their working potential (ca. 3.5 vs. $Li/Li^+$) and high thermal stability [5,6]. In previously reported LPBs with $LiFePO_4$ cathodes, high capacity was observed only at high temperature and low current density, such as $0.05\,mA\,cm^{-2}$ [7]. The SPE can be formed as a thin and shock-absorbable separator. In addition, the charge–discharge performance of LPBs is highly restricted by the interfacial resistance between the electrode and the SPE [8,9].

The interfacial resistance between an electrode and SPE is generally measured using AC impedance spectroscopy with a Li/SPE/cathode half cell. However, the spectrum is observed as a complex resistance, because the impedance includes the resistance of the lithium metal electrode surface and the complicated structure of the composite cathode, which includes SPE and the active electrode material [10–12].

In our previous work [13–15], we have reported the interfacial properties between $LiFePO_4$-C and PEO-LiTFSI using an $Al/Li_{1-x}FePO_4$-C/SPE/$Li_{1-x}FePO_4$-C/Al symmetrical cell with a third stainless steel mesh electrode. There were four major resistance components in the measured impedance spectra (R0–3); the resistances of the PEO-LiTFSI electrolyte (R0–1) and the interfacial resistance between $LiFePO_4$-C and PEO-LiTFSI (R3) were assigned; however, one resistance component, observed in the medium frequency range in the impedance spectrum, has not yet been assigned. In this report, the medium frequency range resistance component was investigated using a symmetrical cell with composite electrodes including $LiFePO_4$-C, $LiCoO_2$, and $LiMn_2O_4$ active materials and $SiO_2$ as an inactive material. An electron blocking cell was also prepared and the resistance was measured in the temperature range of 30–60 °C to con-

---

* Corresponding author. Tel.: +81 59 231 9420; fax: +81 59 231 9478.
*E-mail address:* hanai@chem.mie-u.ac.jp (K. Hanai).

0378-7753/$ – see front matter © 2010 Elsevier B.V. All rights reserved.
doi:10.1016/j.jpowsour.2010.10.079

firm the effect of the electrode thickness and the electrode composition.

## 2. Experimental

The PEO based electrolyte was prepared according to a previously reported solvent casting technique using acetonitrile (AN) as a solvent [16]. PEO (Aldrich Chemical, average molecular weight $6 \times 10^5$) and LiTFSI (Wako) were dissolved in AN with a molar ratio of Li/O = 1/10. The polymer electrolyte solution was cast in a polytetrafluoroethylene (PTFE) dish under a dry argon atmosphere. After evaporation of AN at room temperature, the film was dried at 110 °C for 12 h under vacuum. The thicknesses of the polymer electrolytes used for AC impedance measurements were ca. 500 μm.

The cast type composite cathodes were prepared using $LiFePO_4$-C (Hohsen Co., carbon content 2.0 wt%, average particle size 3.3 μm), $LiCoO_2$ (Hohsen Co., average particle size 12 μm), and $LiMn_2O_4$ (Hohsen Co., average particle size 10.6 μm) active materials, and $SiO_2$ (Kojundo Chemical Lab. Co., Ltd., average particle size 4 μm). The electrodes consisted of the active material, vapor grown carbon fiber (VGCF; Showa Denko, Japan, average diameter 150 nm, length ca. 20 μm) and PEO-LiTFSI mixed in AN ($LiFePO_4$-C:VGCF = 4:1 weight ratio). The solution was painted on aluminum foil and the AN solvent was allowed to slowly evaporate at room temperature under a dry argon atmosphere, followed by drying at 110 °C for 12 h under vacuum. The electrode thicknesses were in the range of 40–60 μm ($LiFePO_4$-C and $SiO_2$-based: ca. 40 μm; $LiCoO_2$ and $LiMn_2O_4$-based: ca. 60 μm) and the active electrode area was 2.25 $cm^2$ (1.5 cm × 1.5 cm). A reversible capacity of 140 mAh $g^{-1}$ at 50 °C was observed for a Li/PEO-LiTFSI/$LiFePO_4$-C cell, which is comparable with the capacity obtained for Li/EC-DEC-$LiClO_4$/$LiFePO_4$-C at room temperature.

A symmetrical cell was used to measure the interfacial resistance between the electrolyte and the electrode (two-probe tests). The lithium content in $Li_xFePO_4$ was changed using a Al/$Li_xFePO_4$-C/PEO-LiTFSI/SS-mesh/PEO-LiTFSI/$Li_xFePO_4$-C/Al cell (SS: stainless steel). The cell was assembled with two $Li_xFePO_4$-C electrodes arranged face to face, as shown in Fig. 1a. A constant current was passed between the SS-mesh and the Al foil as a current corrector to deposit Li metal on the SS-mesh. The Al/electrode/SPE/electrode/Al symmetrical cell was prepared to measure the interfacial resistance between the SPE and the $SiO_2$, $LiCoO_2$ and $LiMn_2O_4$-based electrodes.

The electrode film for the electron blocking cell consisted of $LiFePO_4$-C, VGCF and PEO-LiTFSI mixed in AN ($LiFePO_4$-C:VGCF = 4:1 weight ratio). The solution was cast in a PTFE dish under a dry argon atmosphere. After evaporation of AN at room temperature, the film was dried at 110 °C for 12 h under vacuum. The resulting film was hot-pressed in a PTFE case at 90 °C under vacuum by applying pressure to obtain a homogeneous cathode film. The electrode film thickness was in a range of 120–400 μm and the active electrode area was 0.95 $cm^2$ (1.1 cm diameter).

The electron blocking symmetrical cell was assembled using two lithium metal reference electrodes arranged face to face and the composite electrode located at the center of the cell, as shown in Fig. 1b (four-probe tests).

AC impedance measurements of the composite electrode were performed in the temperature range of 30–60 °C. An AC perturbation of 10 mV was applied in the frequency range from $1 \times 10^6$ to 0.1 Hz using a Solartron 1260 frequency response analyzer. In order to ensure good contact between the electrolyte and electrode, the cells were initially heated to 80 °C and then cooled down to the measurement temperature.

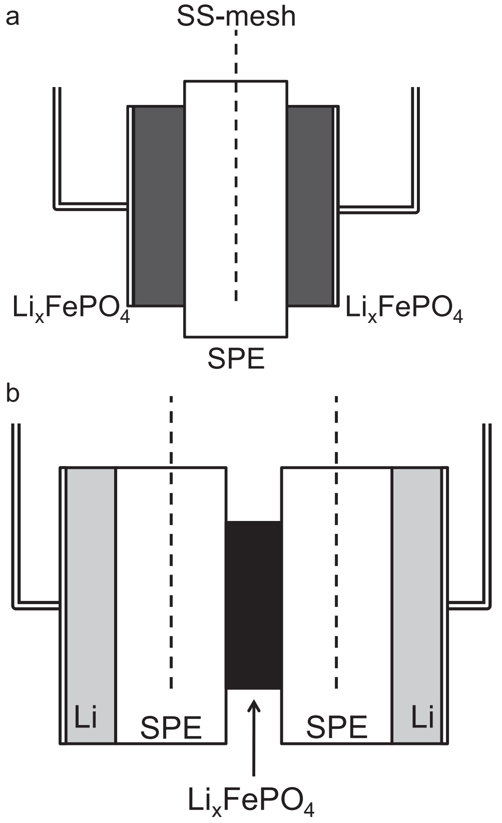

**Fig. 1.** Schematic representations of symmetrical cells. (a) Symmetrical cell with a third stainless steel-mesh electrode (two-probe tests). (b) Electron blocking cell (four-probe tests).

## 3. Results and discussion

Fig. 2 shows the impedance spectrum of a symmetrical cell (Al/$Li_{0.98}FePO_4$-C/PEO-LiTFSI/$Li_{0.98}FePO_4$-C/Al) at 50 °C, in which there are four major resistance components. In our previous report, the simple ohmic resistance (R0) and the resistance in the high frequency range (small semicircle, R1) were assigned to the resistance

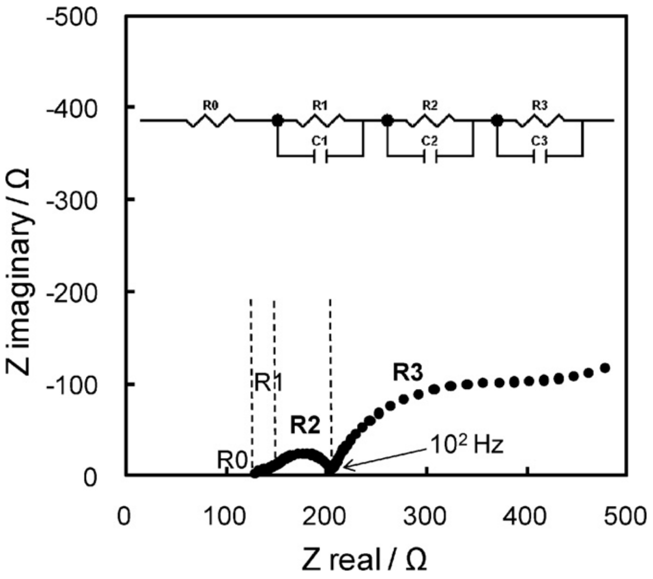

**Fig. 2.** Impedance spectrum for the Al/$Li_{0.98}FePO_4$/SPE/$Li_{0.98}FePO_4$/Al cell measured at 50 °C.

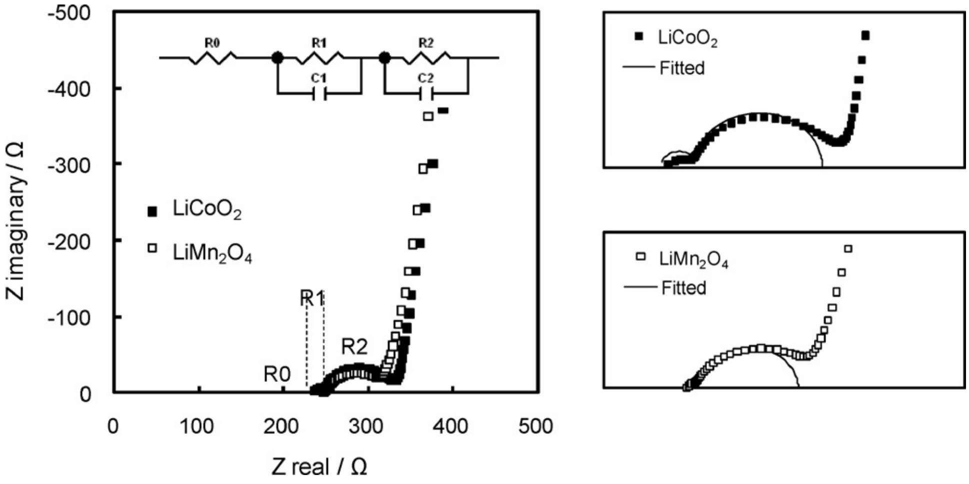

**Fig. 3.** Impedance spectra for the Al/$LiCoO_2$/SPE/$LiCoO_2$/Al and Al/$LiMn_2O_4$/SPE/$LiMn_2O_4$/Al cells measured at 40 °C.

of the PEO electrolyte by comparison with a Cu/PEO-LiTFSI/Cu cell. R3 was affected by the lithium content of $Li_xFePO_4$, and the compositional dependence exhibited a reversible change. The activation energy of R3 was not affected by the change in the conductivity of PEO-LiTFSI due to the crystallization of the PEO. Therefore, R3 has been concluded to be a charge transfer resistance between $LiFePO_4$ and the solid electrolyte interface (SEI) layer. On the other hand, the conductivity profile of R2 was similar to the PEO-LiTFSI electrolyte, and a symmetrical cell with a sputtered thin film electrode did not show the R2 resistance component in the impedance spectrum. Therefore, R2 has been considered to be an internal resistance of the $LiFePO_4$-polymer electrolyte composite electrode.

To confirm the origin of R2, there are two major components that should be tested; the carbon coating in $LiFePO_4$-C and the conductive carbon additive (VGCF). In the liquid electrolyte system, Takahashi et al. [17] reported that the $LiFePO_4$ electrode (with conductive carbon additive) had only one depressed semicircle in the impedance spectrum as the charge transfer process, and Shin et al. [18] reported two depressed semicircle in the impedance spectrum with a carbon-coated $LiFePO_4$ electrode as the lithium ion migration resistance of SEI and the charge transfer process. However, the interfacial property with the polymer electrolyte has not been reported. To confirm the effect of the carbon coating on R2, the dependence of the impedance on the carbon content in $LiFePO_4$-C should be tested. However, the cell with a pure $LiFePO_4$ electrode, the particle size of which was ca. 5 μm, was not suitable for impedance measurement, due to the low conductivity of $LiFePO_4$. In this report, we attempt to examine the effect of the carbon coating using two model electrodes with typical cathode materials ($LiCoO_2$ and $LiMn_2O_4$) and an inactive material ($SiO_2$).

Fig. 3 shows impedance profiles of Al/$LiCoO_2$/PEO-LiTFSI/$LiCoO_2$/Li and Al/$LiMn_2O_4$/PEO-LiTFSI/$LiMn_2O_4$/Li cells at 40 °C, in which they exhibit blocking behavior with a vertical spike, a simple ohmic resistance and two semicircles are observed. Saturation of these structures with lithium ions is indicated by the blocking characteristic. The frequency ranges of these semicircles are similar to those of R1 and R2 for the cell with the $LiFePO_4$-C composite electrode shown in Fig. 2. The resistance component (R2) for the symmetrical cells with $LiCoO_2$ and $LiMn_2O_4$ composite electrodes was obtained by fitting the experimental data using the equivalent circuit shown in Fig. 3, and the temperature dependence of R2 is shown in Fig. 4. The dependence of both cells was similar to the cell with the $LiFePO_4$-C composite electrode. The activation energies for the $LiCoO_2$ and $LiMn_2O_4$ composite electrodes were calculated as 14 kJ mol$^{-1}$ and 20 kJ mol$^{-1}$, respectively. These values are comparable to that for the cell with the $LiFePO_4$-C composite electrode, which suggests that the coating carbon does not affect the impedance profiles. The composite electrode contains a conductive carbon additive which contacts with active material particle. The lithium ion migration resistance of the carbon should be assigned in the impedance spectrum. Appetecchi et al. [19,20] reported the impedance profile of the composite electrode with $LiMn_2O_4$. In their study, ion transportation in the PEO electrolyte with a conductive carbon powder was similar to that for the pure electrolyte, and the charge transfer process was only attributed to the active material.

To clarify the effect of the active material in the composite electrode, the cell impedance was measured using an inactive material for the charge–discharge reaction as a model electrode. Some ceramic nanofiller materials have been studied to improve the ion transport ability of the PEO electrolyte and the surface stability between a lithium metal electrode and the electrolyte [21]. On the other hand, Johansson et al. [22] observed little increase of conductivity upon the addition of fumed silica to PEO-LiTFSI electrolyte. Therefore, $SiO_2$ particles are expected

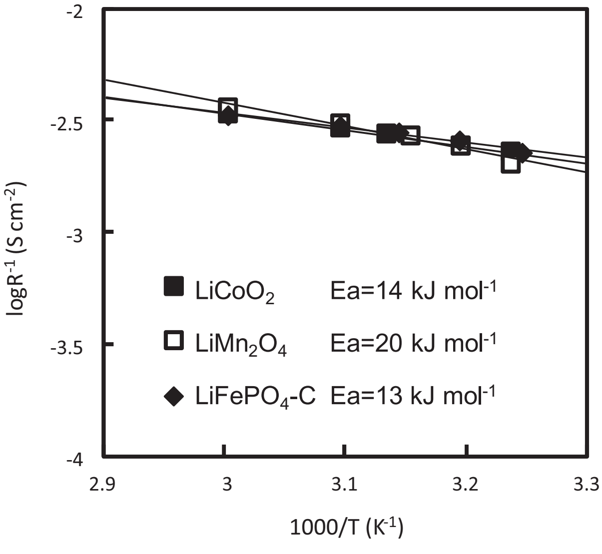

**Fig. 4.** Temperature dependence of the R2 interface resistance measured for different composite electrodes ($LiCoO_2$ and $LiMn_2O_4$).

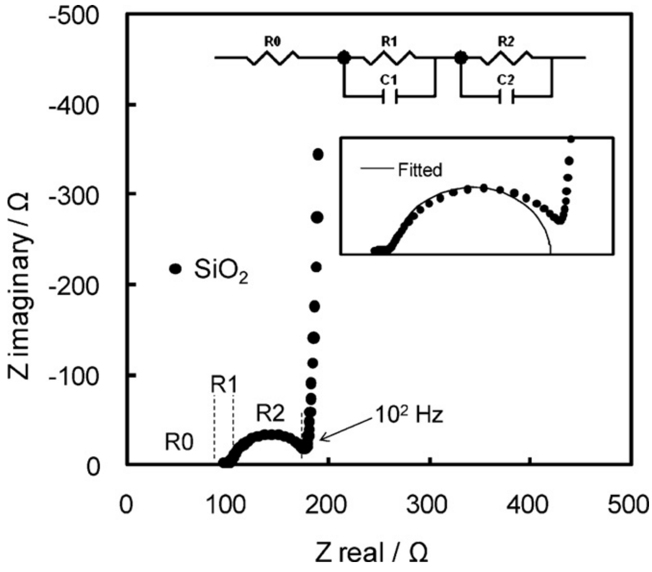

**Fig. 5.** Impedance spectrum for the Al/SiO$_2$/SPE/SiO$_2$/Al cell at 40 °C.

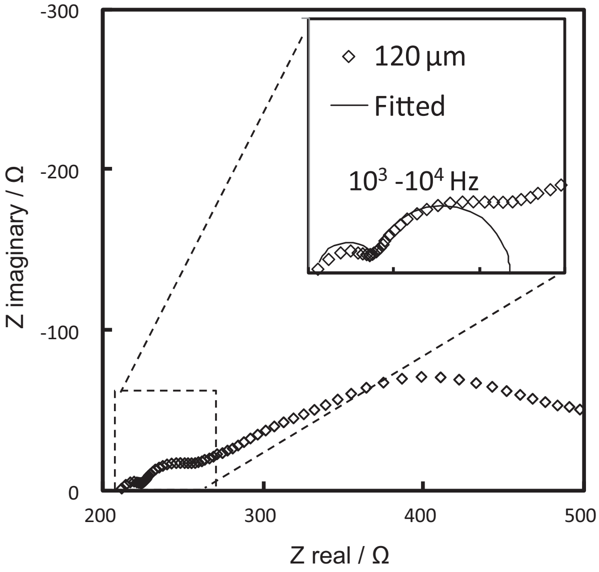

**Fig. 7.** Impedance spectrum for the Cu/Li/SPE/LiFePO$_4$-C/SPE/Li/Cu electron blocking cell at 50 °C.

to be a suitable material for preparation of the inactive model electrode.

Fig. 5 shows the impedance profile for the Al/SiO$_2$/PEO-LiTFSI/SiO$_2$/Al cell using micrometer-sized SiO$_2$ particles, measured at 40 °C. The symmetrical cell with the model electrode exhibits blocking behavior with a vertical spike, and only two semicircles, R1 and R2, are observed, which indicates that SiO$_2$ is an inactive material for the electrochemical reaction. The frequency ranges of these semicircles were similar to those of R1 and R2 for the LiFePO$_4$-C composite electrode cell shown in Fig. 2. The resistance value of R2 was obtained by fitting the experimental data using the equivalent circuit shown in Fig. 5. An Arrhenius plot of the R2 resistance for the model electrode is shown in Fig. 6. The temperature dependence of R2 exhibits the same profile as the composite electrode cell shown in Fig. 4. The activation energy for R2 of the model electrode was calculated as 8 kJ mol$^{-1}$ from the temperature dependence in the measurement range, which is comparable to that for the LiFePO$_4$-C composite electrode cell. This result indicates that R2 is not affected by carbon coating of the active materials.

The composite electrode also contains VGCF as a conductive carbon additive, which forms a complicated electron network in the electrode. Appetecchi et al. also reported the impedance profile of a polymer electrolyte–carbon composite electrolyte using a two-electrode cell, in which the composite electrode was placed between stainless steel disks. In the report, the composite polymer electrolyte with a large amount of conductive carbon exhibited a small semicircle in the impedance spectrum as an electron-ion mixed conductor.

To clarify the electrochemical reaction in the composite electrode, an electron blocking symmetrical cell was prepared with a LiFePO$_4$-C composite electrode as described in Section 2. Fig. 7 shows the impedance spectrum of the Li/PEO-LiTFSI/LiFePO$_4$-C/PEO-LiTFSI/Li cell at 50 °C, in which there are four major

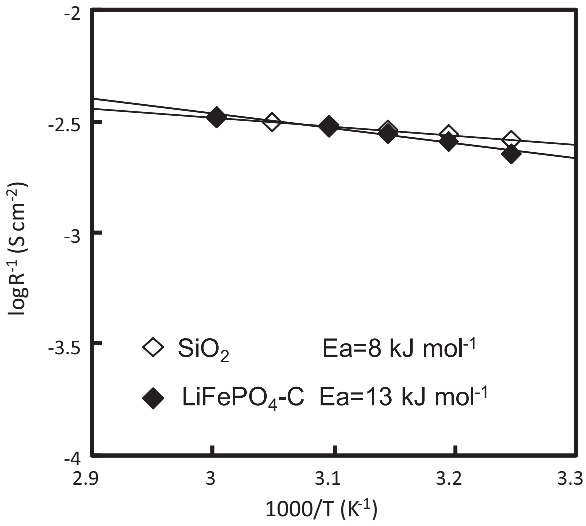

**Fig. 6.** Temperature dependence of the R2 interface resistance measured for the SiO$_2$ composite electrode.

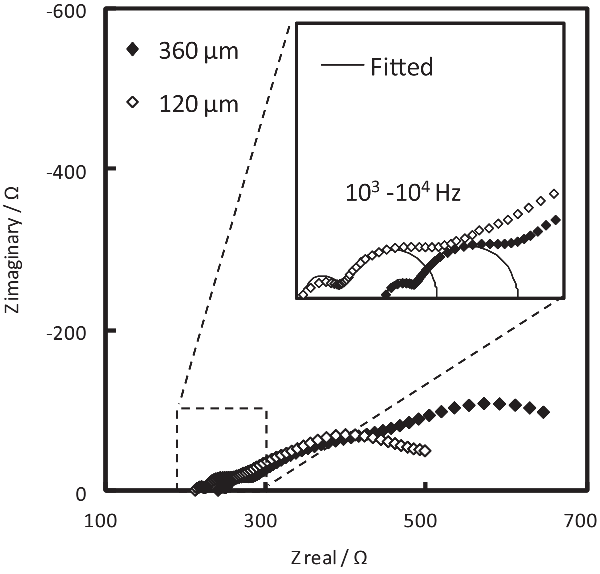

**Fig. 8.** Impedance spectra for Cu/Li/SPE/LiFePO$_4$/SPE/Li/Cu electron blocking cells with 120 and 360 µm thick composite electrodes.

**Table 1**
Dependence of the interface resistance and activation energy on the electrode thickness for the composite electrode of $LiFePO_4$-VGCF:SPE (60:40 weight ratio) in the temperature range of 40–60 °C.

| Thickness (μm) | Resistance (50 °C) R2 (Ω) | Activation energy (40–60 °C) R2 ($kJ\,mol^{-1}$) |
|---|---|---|
| 120 | 42 | 53 |
| 350 | 46 | 49 |

**Table 2**
Dependence of the interface resistance and the activation energy on the electrode composition for composite electrode of $LiFePO_4$-VGCF-SPE.

| Electrode composition ($LiFePO_4$-VGCF):SPE | Electrode properties | | Resistance (60 °C) R2 (Ω) | Activation energy (40–60 °C) R2 ($kJ\,mol^{-1}$) |
|---|---|---|---|---|
| | Thickness (μm) | Weight ($mg\,cm^{-2}$) | | |
| 40:60 | 360 | 67 | 32 | 43 |
| 50:50 | 360 | 73 | 29 | 53 |
| 60:40 | 350 | 75 | 25 | 49 |
| 80:20 | 400 | 94 | 24 | 50 |

resistance components. The small semicircle in the high frequency range and the semicircle in the medium frequency range are similar to that of R1 and R2 for the $LiFePO_4$-C composite electrode cell shown in Fig. 2. The depressed semicircle in the low frequency range is considered to be the resistance of ion transportation, in which lithium ions pass through the composite electrode film. The resistance component corresponding to the charge transfer resistance between the polymer electrolyte and $LiFePO_4$-C, R3, was not observed in the impedance spectrum. There is no electron pass from the external device into the composite electrode. Therefore, it is considered that R2 is not related to the charge transfer process on the $LiFePO_4$-C/VGCF composite electrode.

The influence of the electrode thickness on the R2 resistance component was examined in the temperature range of 40–65 °C. Fig. 8 shows the impedance profiles of the Cu/Li/PEO-LiTFSI/$LiFePO_4$-C/PEO-LiTFSI/Li/Cu electron blocking cells with 120 and 360 μm thick composite electrodes. The increase in the ohmic resistance is attributed to the thickness of the PEO-LiTFSI electrolyte incorporated into the symmetrical cell. The large depressed semicircle in the low frequency range increases with increasing electrode thickness. On the other hand, the impedance profile of the R2 semicircle is not affected by the thickness of the composite electrode. The resistance and the activation energy of R2 are summarized in Table 1. The resistance and the activation energy for the 360 μm thick composite electrode were comparable to that for the 120 μm thick electrode. This indicates that R2 does not correspond to the lithium ion migration process of the electrode. The interface area between the composite electrode and the polymer electrolyte is not affected by the thickness of the electrode film. Therefore, R2 is considered to be an interfacial resistance of the composite electrode. Johnson et al. [23] reported that the morphology of a PEO-LiTFSI electrolyte film cast from the solution was affected by the substrate material. In their report, the polymer electrolyte film cast onto a substance had different salt concentrations in the bulk and surface of the electrolyte film. Therefore, it is considered that, there are restricted polymer electrolyte layers on the surfaces of the active material particles and the carbon additive, and R2 corresponds to the interfacial resistance between these layers and the electrolyte film.

Decrease of the interfacial resistance of the composite electrode would be exceedingly effective to realize the practical application of all the solid polymer lithium ion battery. To confirm the effect of the surface morphology of the electrode, the influence of the electrode composition on R2 was examined in the temperature range of 30–60 °C and the results are summarized in Table 2. R2 decreases with decreasing PEO-LiTFSI electrolyte content in the composite electrode. However, no significant change in the activation energy was evident with the change in the electrode composition. It is indicated that the property of R2 is not affected by the electrode composition, the value of which is dominated by the ratio of PEO-LiTFSI electrolyte as a frequency factor.

## 4. Conclusion

The interfacial resistance between the composite electrode and PEO-based solid polymer electrolyte was examined by AC impedance measurements of two different symmetrical cells in the temperature range of 30–60 °C. The resistance component obtained in the medium frequency range in the impedance spectrum was observed for symmetrical cells with different cathode materials ($LiFePO_4$-C, $LiCoO_2$, $LiMn_2O_4$ and $SiO_2$). Electron blocking cells were also prepared and measured in the temperature range of 30–60 °C to confirm the effect of the electrode thickness and the electrode composition.

The values of resistance and activation energy were not affected by the thickness of the composite electrode. Therefore, the resistance was assigned to an interfacial resistance between the composite electrode and the PEO-LiTFSI electrolyte. The resistance was affected to the electrode composition, which decreased with decreasing PEO-LiTFSI electrolyte content in the composite electrode.

## Acknowledgement

This study was supported by the Cooperation of Innovative Technology and Advanced Research in Evolution Area (City Area) Project of the Ministry of Education, Sports, Science and Technology of Japan.

## References

[1] M. Gauthier, D. Fauteux, G. Vassort, A. Bélanger, M. Duval, P. Ricoux, J.-M. Chabagno, D. Muller, P. Rigaud, M.B. Armand, D. Deroo, J. Electrochem. Soc. 132 (1985) 1333–1340.
[2] Y. Kobayashi, S. Seki, Y. Mita, Y. Ohno, H. Miyashiro, P. Charest, A. Guerfi, K. Zaghib, J. Power Sources 185 (2008) 542–548.
[3] J.W. Fergus, J. Power Sources 195 (2010) 4554–4569.
[4] Y. Xia, K. Tatsumi, T. Fujieda, P.P. Prosini, T. Sakai, J. Electrochem. Soc. 147 (2000) 2050–2056.
[5] F. Croce, F.S. Fiory, L. Persi, B. Scrosati, Electrochem. Solid-State Lett. 4 (2001) A121–A123.
[6] L. Damen, J. Hassoun, M. Mastragostino, B. Scrosati, J. Power Sources 195 (2010) 6902–6904.
[7] G.B. Appetecchi, J. Hassoun, B. Scrosati, F. Croce, F. Cassel, M. Salomon, J. Power Sources 124 (2003) 246–253.
[8] Q. Li, T. Itoh, N. Imanishi, A. Hirano, Y. Takeda, O. Yamamoto, Solid State Ionics 159 (2003) 97–109.
[9] Q. Li, N. Imanishi, Y. Takeda, A. Hirano, O. Yamamoto, Electrochem. Solid-State Lett. 7 (2004) A470–A473.
[10] Y. Masuda, M. Nakayama, M. Wakihara, Solid State Ionics 178 (2007) 981–986.
[11] C. Koga, S. Wada, M. Nakayama, Electrochim. Acta 55 (2010) 2561–2566.
[12] D. Saito, Y. Ito, K. Hanai, T. Kobayashi, N. Imanishi, A. Hirano, Y. Takeda, O. Yamamoto, J. Power Sources 195 (2010) 6172–6176.
[13] K. Hanai, T. Matsumura, N. Imanishi, A. Hirano, Y. Takeda, O. Yamamoto, J. Power Sources 178 (2008) 789–794.
[14] K. Hanai, R. Uchiyama, N. Imanishi, A. Hirano, Y. Takeda, O. Yamamoto, J. Jpn. Soc. Powder Powder Metallurgy 56 (2009) 71–75.

[15] K. Hanai, K. Kusagawa, M. Ueno, T. Kobayashi, N. Imanishi, A. Hirano, Y. Takeda, O. Yamamoto, J. Power Sources 195 (2010) 2956–2960.
[16] C. Capiglia, J. Yang, N. Imanishi, A. Hirano, Y. Takeda, O. Yamamoto, J. Power Sources 119–121 (2003) 826–832.
[17] M. Takahashi, S. Tobishima, K. Takei, Y. Sakurai, Solid State Ionics 148 (2002) 283–289.
[18] H.C. Shin, W.I. Cho, H. Jang, Electrochim. Acta 52 (2006) 1472–1476.
[19] G.B. Appetecchi, M. Carewska, F. Alessandrini, P.P. Prosini, S. Passerini, J. Electrochem. Soc. 147 (2000) 451–459.
[20] G.B. Appetecchi, S. Passerini, Electrochim. Acta 45 (2000) 2139–2145.
[21] F. Croce, G.B. Appetecchi, L. Persi, B. Scrosati, Nature 394 (1998) 456–458.
[22] P. Johansson, M.A. Ratner, D.F. Shriver, J. Phys. Chem. B 105 (2001) 9016–9021.
[23] P.L. Johnson, M.W. Kennedy, C.M. Smith, N. Truong, D. Teeters, Electrochim. Acta 53 (2007) 1490–1496.